
Ultrasound Imaging Techniques and Procedures

Stefano Bianchi, René de Gautard, Giorgio Tamborrini, and Stefan Mariacher

Contents

1	Introduction	65
2	Technique of Examination and Normal US Appearance	66
3	Dorsal Aspect	67
4	Palmar Aspect	72
5	Key Points	75
5.1	Advantages of Ultrasound in Wrist and Hand Assessment.....	75
5.2	Disadvantages of Ultrasound in Wrist and Hand Assessment.....	77
5.3	Operator Requisites for US Examination in Wrist and Hand Assessment.....	77
5.4	Basic Principles of US Technique of Examination in Wrist and Hand Assessment.....	78
	References	78

S. Bianchi (✉) · R. de Gautard
CIM SA Cabinet Imagerie Medicale,
Route de Malagnou 40, 1208 Geneva, Switzerland
e-mail: stefanobianchi@bluewin.ch

G. Tamborrini
Rheumaklinik, Universitäts-Spital Zürich,
Rämi-Strasse 100, 8091 Zürich, Switzerland

S. Mariacher
Chefarzt und stv. Vorsitzender der Klinikleitung,
aarReha Schinznach, Badstrasse 55P,
5116 Schinznach-Bad, Switzerland

S. Bianchi
Clinique des Grangettes, Chemin de Grangettes 7, 1224
Geneva, Switzerland

Abstract

The role of ultrasound (US) in the assessment of musculoskeletal disorders is persistently increasing. Recent developments in hardware and software of US equipments and in particular use of small-size, high-frequency transducers have allowed accurate assessment of a wide variety of hand and wrist disorders.

1 Introduction

The role of ultrasound (US) in the assessment of musculoskeletal disorders is persistently increasing (Van Holsbeeck and Introcaso 2001; Mc Nally 2004; Brasseur and Tardieu 2006; Bianchi and Martinoli 2007). Recent developments in hardware and software of US equipments and in particular use of small-size, high-frequency transducers have allowed accurate assessment of a wide variety of hand and wrist disorders. The main advantages of US are its low cost, readiness, non invasivity and possibility to perform a dynamic examination. The main disadvantage is the impossibility to detect and assess deep structures, located behind bones. In addition, US is a highly operator-dependent technique and has a long learning curve. US has been used in the assessment of wrist and hand traumatic, degenerative and infective disorders, as well as in evaluating local masses (Read et al. 1996; Ferrara and Marcellis 1997; Bianchi et al. 1999, 2001, 2003; Teefey et al. 2000; Milbradt et al. 1990; Chiou et al. 2001; Moschilla and Bredahl 2002). Additional studies have stressed its role in the evaluation of inflammatory arthritis (Koski 1992; Grassi et al. 1993).

Quantification of inflammation and of structural damage is mandatory in the assessment, management and monitoring of rheumatoid arthritis (RA). Without appropriate treatment (e.g. DMARD's, biologics), RA inflammation can progress and result in joint dysfunction and deformity. An early diagnosis can lead to early instauration of a successful treatment. Standard radiographs have an important role to identify changes such as osteopenia, joint space reduction or erosions in patients with advanced arthritis. US is a useful tool in the assessment and follow-up of early to established RA (Wakefield et al. 2000, Szkudlarek et al. Szkudlarek et al. 2004a, b) and can efficiently guide local procedures such as aspiration of effusions or therapeutic injection (Karim et al. 2001). In RA US can detect different pathologic changes including synovitis, cartilage and bone changes, tenosynovitis and tendon tears, bursitis, rheumatoid nodules or secondary nerve entrapment (e.g. carpal tunnel syndrome). Clinical studies have shown that US is as effective or even more effective in detecting inflammatory changes as clinical examination. Sensitivity and specificity of US in assessment of joints changes in RA is comparable to MR imaging (Backhaus et al. 1999; Backhaus et al. 2002; Szkudlarek et al. 2004a, b; Scheel et al. 2006). Power Doppler and Colour Doppler US detects active synovial inflammation associated with hypervascularisation and neoangiogenesis. In the presence of an active synovitis, there is an increase in signal activity, which is correlated to the degree of inflammatory activity. Therefore, the use of color and power Doppler US facilitates a differentiation between active and inactive synovitis. Furthermore, numerous studies have shown a good correlation between activity of synovitis at power Doppler and inflammatory changes evident at MRI and at histopathology studies (Walther et al. 2001; Terslev et al. 2003). Echo-contrast-enhanced US has shown an improvement in the measurement of synovial thickness and activity of synovial processes in patients with rheumatoid arthritis and allows better differentiation between effusion and synovial proliferation (Goldberg et al. 1994; Blomley et al. 2001). Besides assessment of the synovium, US can evaluate pathological changes of cartilages and bones if performed using high-resolution ultrasound probes. Bone erosions are a pathophysiological hallmark of RA. US can provide a more accurate and comprehensive assessment of bone erosions than

plain radiography. The size of erosions can be monitored to evaluate disease progression.

Accurate knowledge of the normal anatomy, technique of US examination and of the US appearance of the hand and wrist are definite pre-requisites for a successful US examination. The target of this chapter is to present the technique of the US examination and the normal US anatomy of the hand and wrist.

2 Technique of Examination and Normal US Appearance

Before starting the US examination, any previous imaging studies and blood tests, if available, are reviewed. Every effort must be made to obtain a recent radiographic examination, in at least two perpendicular views, since this allows a good analysis of joints and bones and is complementary to US that permit an excellent assessment of most soft tissues. A brief clinical evaluation is always obtained since it helps in pointing the attention of the examiner to a specific area, thus shortening the time of examination and allowing a more detailed local assessment. The patient is asked for duration of symptoms, type and rhythm of pain (mechanic or inflammatory), presence of tingling, numbness or morning stiffness. If pain is the main symptom, its location and modification during muscle contraction or joint movements can often orient toward the correct diagnosis. In De Quervain tenosynovitis, for example, a sharp, acute pain located over the radial styloid and worsened by ulnar deviation of the wrist with the thumb flexed is highly suggestive of the diagnosis. The distribution of peripheral tingling can indicate the injured nerve (radial, ulnar or median). A brief regional physical examination including assessment of any local or diffuse swelling, warm or reddens follows. The joint range of motion and local tenderness are also briefly assessed.

Schematically, there are two main kinds of performing a US examination of the wrist and hand. A *focused examination* generally performed in patients suffering from disorders affecting the periarticular tissues and a *systemic examination* mostly directed to the joints. The first is a shorter examination concentrated on a specific region, selected by the sonologist according to the data available from the physician's US request, type of symptoms and results of the brief clinical examination described earlier. We perform this

type of examination in the vast majority of our patients. To give an example in a patient presenting with a painless lump at the dorsum of the wrist suspected to be a ganglion by the referring physician, the US examination can be limited to the dorsal aspect of the wrist. A time-consuming, detailed examination of all metacarpophalangeal and interphalangeal joints is not necessary and useless in such a patient. The second type of US examination is a more time-consuming, systematic examination usually obtained only in patients with a clinical suspicion or diagnosis of systemic arthritis. In both cases, a scrupulous technique of realization of the US examination, including images obtained in several planes and dynamic test, must be deployed (Creteur and Peetrons 2000; Middleton et al. 2001; Lee and Healy 2005; Tagliafico et al. 2007).

For didactic purposes, we first describe the basic anatomy of the main structures amenable to US assessment followed by description of the US technique of examination and of the normal US anatomy. We will follow an anatomic pattern, starting with the dorsal aspect of the wrist and the hand followed by the palmar aspect.

For optimal US examination of the wrist and hand, the patient sat facing the examiner with the forearm resting on the examination bed. We routinely start the examination by scanning the dorsal aspect of the wrist followed by the hand through transverse and sagittal sonograms. Then, the patient is asked to supinate the hand that now lies on its dorsal aspect, to allow examination of its palmar aspect. Again transverse sonograms are followed by longitudinal images. Color Doppler is routinely obtained. Dynamic scanning allows identification of each extensor and flexor tendon of the fingers and, most importantly, allows optimal judgement of tendons' gliding and eventual impingement inside osteofibrous tunnels. This is very useful in judging presence of tendons adhesions. Application of variable pressure with the transducer permits obtaining additional data. A firm pressure helps in eliciting local pain and thus in focalizing the examination. It also assists in judging consistency of masses facilitating for example the diagnosis of soft tissue lipoma. On the contrary, large amount of gel must be used in assessing fluid collections in order to lessen local pressure through the probe and avoid inadvertent displacement of the fluid that can result in a negative examination. In assessing presence of vessels with color Doppler, excessive pressure can

result in squeezing of vessels resulting in impossibility to accurately detect local hypervascular changes. In testing the permeability of subcutaneous veins, color Doppler is obtained during squeezing of the soft tissues distal to the site of examination performed with the contralateral hand of the examiner. This allows a temporary increase in venous blood velocity and its easier detection at color Doppler. On the contrary, blocking the venous drainage at the forearm causes dilatation of the distal vein and results in stagnation of blood inside venous masses. As previously discussed, palpation under US guidance can be realized through the transducer when a large mass is evaluated. When the mass is small, US-guided palpation is better performed by using an opened paper clip. Once placed between the transducer and the skin, this can be followed under real-time scanning thanks to its typical posterior comet tail artifact. This technique works well in cutaneous marking of soft tissue foreign bodies as well as in accurate localization of small neuromas.

3 Dorsal Aspect

US allows an accurate evaluation of the dorsal aspect of wrist and hand (Figs. 1, 2, 3, 4, 5, 6, 7, 8). Accessory muscles can be found at the dorsal face of the wrist (Muncibì et al. 2008) as anatomic variants mimicking local tumors. They show at US the typical internal muscle structure made by alternating hypoechoic (muscle fibers) and hyperechoic (fibroadipose septa) bands. Dynamic examination during resisted contraction shows contraction of the accessory muscle thus confirming the diagnosis. Located under the skin and subcutaneous tissues, a thin fascia covers the extensor tendons (ET). These tendons origin from the miotendineous junctions, located in the forearm at different level for each muscle, run distally between the joint plane and the subcutaneous tissue, to finally insert into the bone of the wrist and hand. Since all ET change their course before joining their insertion, they are prone to instability during changes of position of the wrist and hand joints. To avoid instability, the ET run inside fibrous tunnels. These are made by the surface of bones covered by periosteum (the floor) and by superficial fibrous bands named retinacula (the ceiling). To further increase tendons stability, the bone surface is not flat but made by grooves, sulci or protuberances. A synovial sheath composed by a visceral and parietal

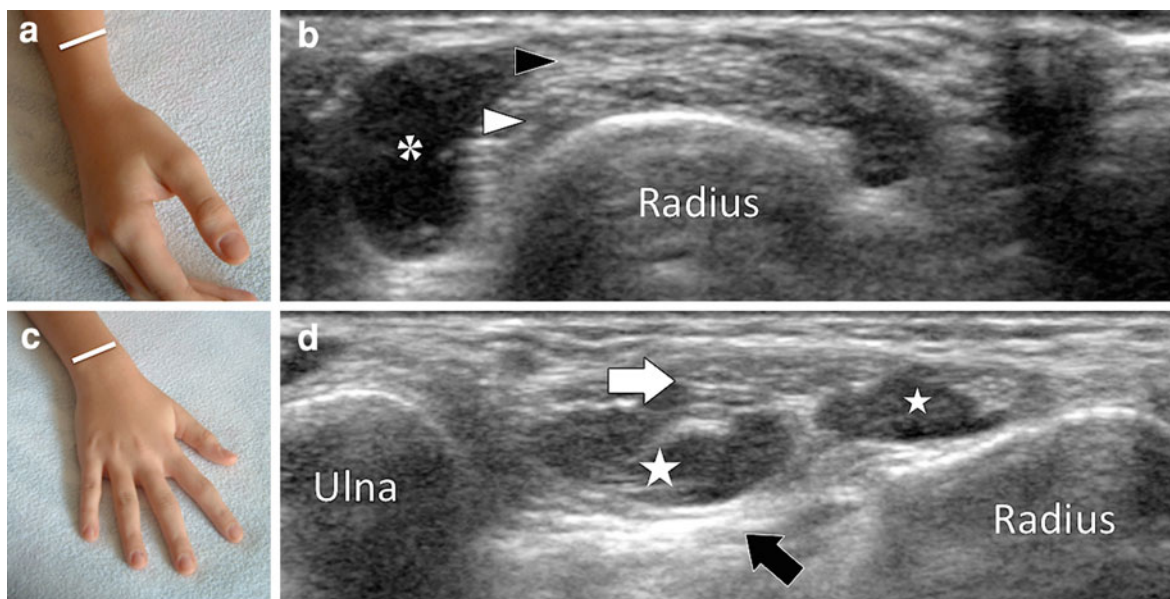
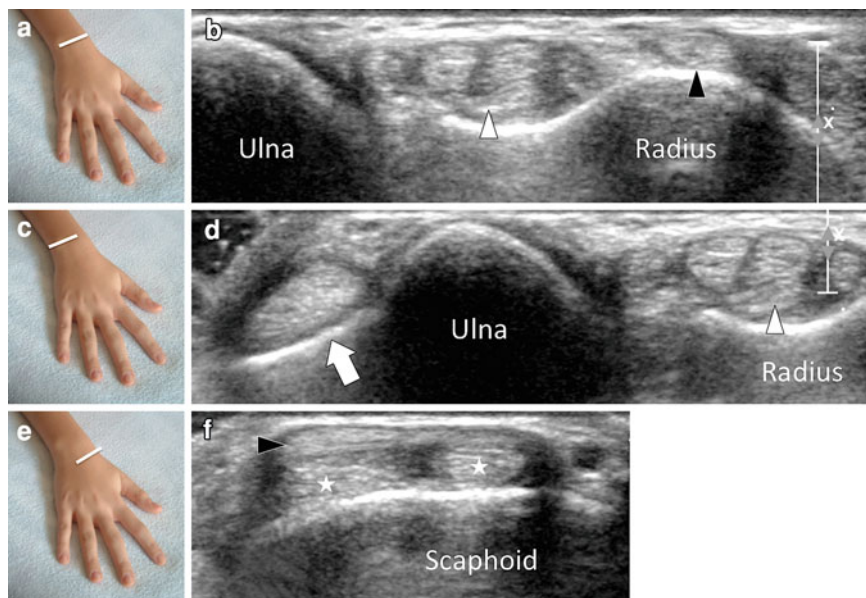


Fig. 1 Dorsal aspect. **a, c** Probe positioning for transverse examination. **b** Sonogram obtained as shown in **a**. US shows the crossing of the tendon of the first extensor compartment (*black arrowhead*) over those of the second compartment (*white arrowhead*). Asterisk distal part of the muscle of the first extensor compartment. **d** Sonogram obtained as shown in **c**.

US shows the miotendineous junctions of the extensor pollicis longus (*small star*) and extensor indicis proprius (*large star*). The extensor digitorum communis tendons (*white arrow*) are located more superficially. Note the interosseous membrane (*black arrow*) appearing as a hyechogenic structure connecting the ulna and the radius

Fig. 2 Dorsal aspect. **a, c, e** Probe positioning for transverse examination. **b, d, f** corresponding sonograms. **b** *White arrowhead* extensor digitorum communis tendons, *black arrowhead* extensor pollicis longus tendon. **d** *White arrowhead* extensor digitorum communis tendons, *arrow* extensor carpi ulnaris tendon. **f** *Black arrowhead* extensor pollicis longus tendon, *stars* extensor carpi radialis tendons



layer, gliding one over the other, surrounds the tendons and reduces local frictions during gliding. The visceral layer is adherent to the tendon and moves with it, while the parietal layer is lax and blends with the retinacula

and other peritendineous structures. The layers are separated by a thin amount of synovial fluid. At the level of the distal radius and wrist, the twelve ET run inside six tunnels. The tunnels are numbered from the

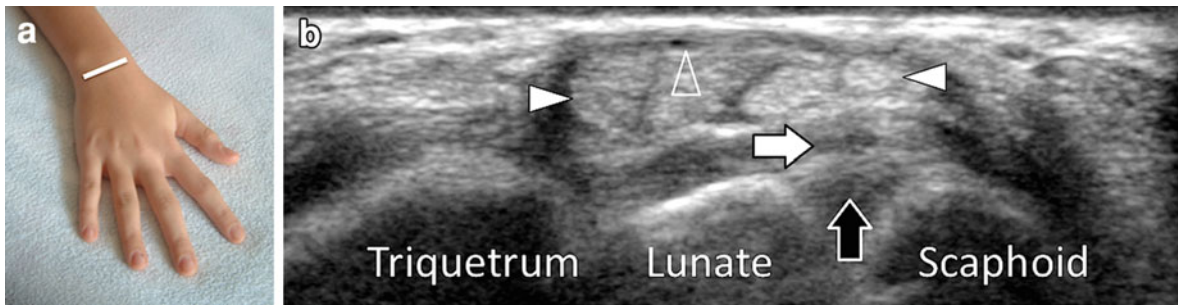


Fig. 3 Dorsal aspect. **a** Probe positioning for transverse examination **b** corresponding sonogram. *White arrowheads* extrinsic dorsal carpal ligaments and radiocarpal synovial space, *black arrow* dorsal band of the scapho-lunate ligament

White arrow extrinsic dorsal carpal ligaments and radiocarpal synovial space, *black arrow* dorsal band of the scapho-lunate ligament

Fig. 4 Dorsal aspect. **a, c** Probe positioning for transverse examination. **b** Sonogram obtained as shown in **a**. *Met* metacarpals, *DIM* dorsal interosseous muscles, *black arrowheads* extensor tendons. **d** Sonogram obtained as shown in **c**. *White arrowheads* extensor indicis proprius and extensor digitorum communis tendon of the index

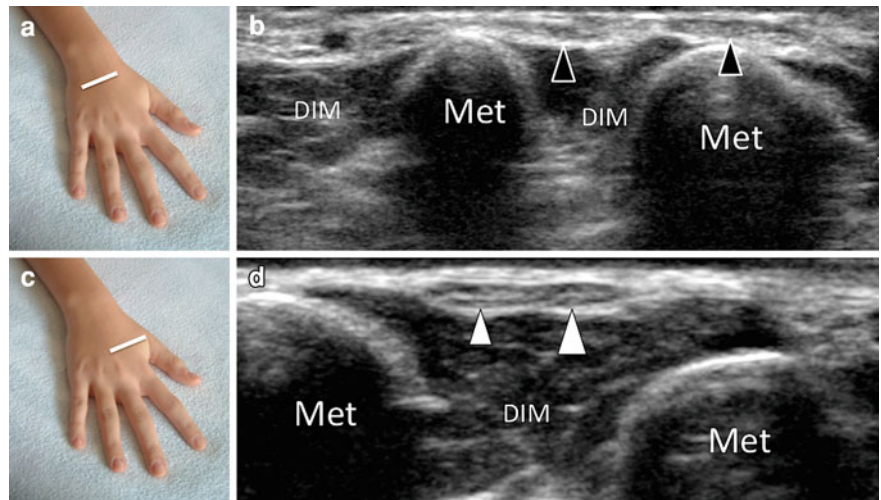


Fig. 5 Dorsal aspect. **a, c** Probe positioning for transverse examination. **b** Sonogram obtained as shown in **a**. *Met* metacarpal, *white arrowhead* extensor digitorum tendon, *asterisks* subcutaneous veins. **d** Sonogram obtained as shown in **c**. *White arrowheads* extensor digitorum communis tendons, *black arrowheads* sagittal bands

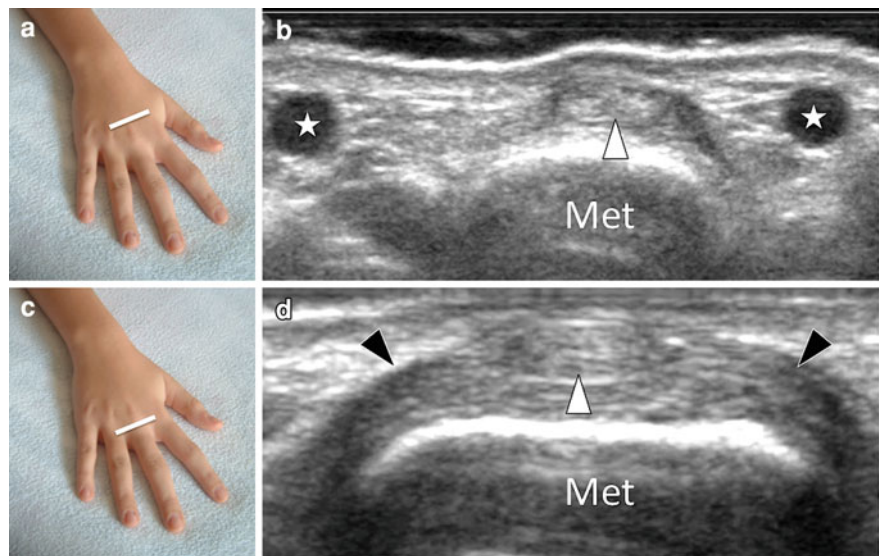


Fig. 6 Dorsal aspect. **a, c, e** Probe positioning for longitudinal examination. **b, d, f** corresponding sonograms. **b** Asterisk triangular fibrocartilage complex, white arrowhead extensor carpi ulnaris tendon, star base of the fifth metacarpal. **d** Black arrowhead extensor digitorum communis tendons, 1 radiocarpal joint, 2 mediocarpal joint. **f** Arrow extensor tendons of the first compartments, RA radial artery

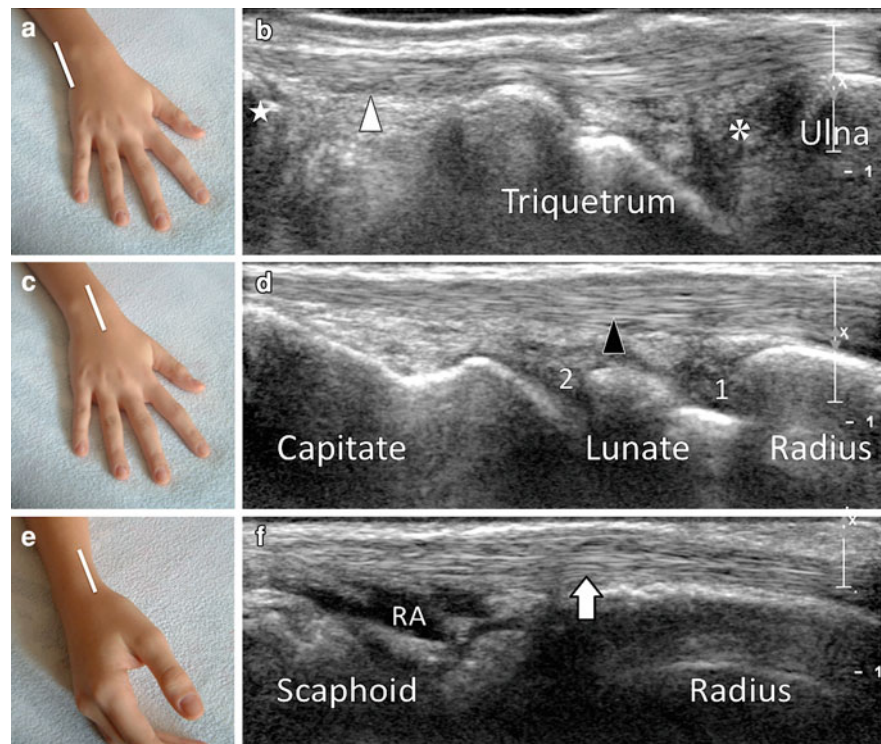
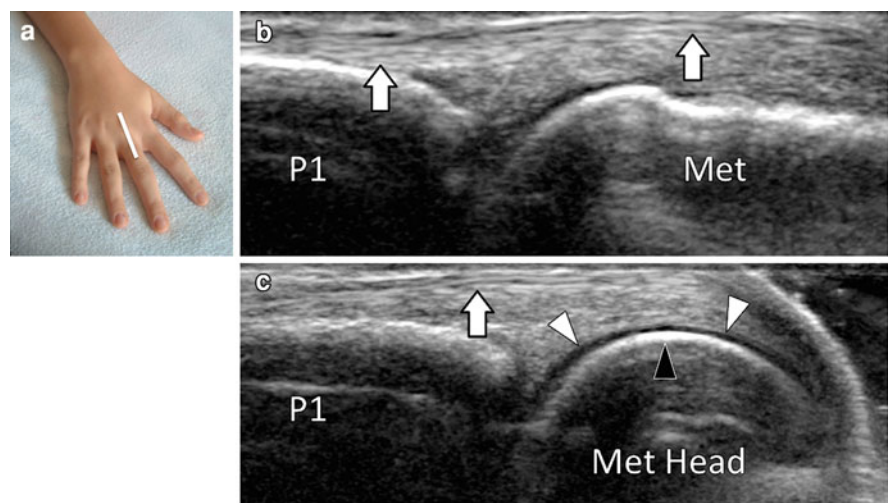


Fig. 7 Dorsal aspect. **a** Probe positioning for longitudinal examination. **b** Sonogram obtained as shown in **a**. **b** Arrows extensor digitorum communis tendon, P1 proximal phalanx. **c** Sonogram obtained with 90° of flexion of the metacarpophalangeal joint. White arrowheads articular cartilage, black arrowhead subchondral bone plate



most radial to the most ulnar. The first tunnel is located over the radial styloid while the sixth is found at the level of the cubital head. Table 1 resumes the arrangement of the tendons inside the six tunnels.

US shows the ET as hyperechoic, homogeneous structures showing a typical fibrillar structure in the longitudinal sonograms. The borders of normal tendons are regular and well defined. The normal

synovial sheath and the tiny amount of fluid contained inside it can't be detected even if high-resolution transducers are used. Retinacula are imaged at US as hyper or hypoechoic structures depending on the incidence of the US beam. They present different thickness depending of the fibroosseous tunnel examined. The retinaculum of the fourth compartment is the thicker and, since it appears mostly

Fig. 8 Dorsal aspect. **a**, **c** Probe positioning for longitudinal and transverse examination. **b** Sonogram obtained as shown in **a**. *1 Met* first metacarpal, *white arrowheads* aponeurosis of the adductor pollicis brevis muscle, *asterisk* ulnar collateral ligament. **d** Sonogram obtained as shown in **c**. *1 Met* first metacarpal, *white arrowheads* aponeurosis of the adductor pollicis brevis muscle, *asterisk* ulnar collateral ligament, *arrow* extensor pollicis longus tendon

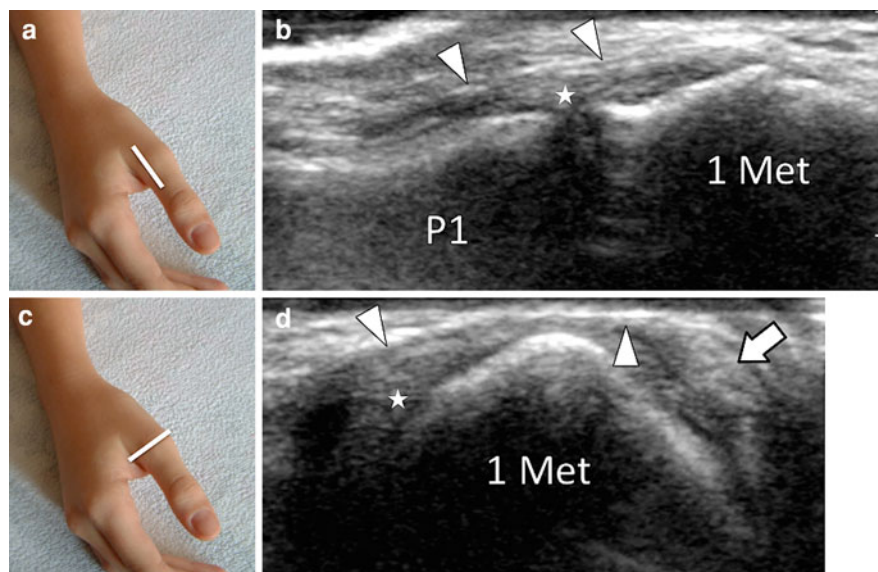


Table 1 Extensor tendons

1 Tunnel = abductor pollicis longus
2 Tunnel = extensor pollicis brevis
3 Tunnel = extensor pollicis longus
4 Tunnel = extensor digitorum communis and extensor indicis proprius
5 Tunnel = extensor digiti minimi
6 Tunnel = extensor carpi ulnaris

hypoechoic, can simulate an effusion to unexperienced examiners (Robertson et al. 2007). The mean value or retinaculas' thickness in other tunnels is around 0.3-0.5 mm. In case of suspicion of mild thickening of retinacula, the contralateral side can be scanned to improve diagnostic confidence. In normal conditions, color Doppler does not allow detecting the normal vascularisation of tendons, sheath or retinacula. Any Doppler signals inside these structures must be retained as pathologic. Axial images allow a good analysis of details of different ET. To give an example, the APL is almost always made by multiple thin tendons rather than by a single tendon (De Maeseneer et al. 2009). This normal variation seems to facilitate impingement inside the first osteofibrous tunnel.

Deep to the ET of the third compartment, located close to the lateral aspect of the Lister's tubercle, the distal sensitive branch of the posterior interosseous nerve can be seen running from the forearm to the dorsal aspect of the wrist. At its distal portion, the

normal nerve can present a bulbous swelling (Acrel's ganglion) that must not be interpreted as a pathologic neuroma or as evidence of chronic compression. The origin of this fusiform swelling is unknown. Histologically, it is made by normal peripheral nerve structures without any neuronal cell bodies (Tubbs et al. 2007). The term pseudoganglion seems then more appropriate than that of ganglion. In younger subjects, a small artery (distal anterior interosseous artery) can be detected running close to the nerve. The distal radio-ulnar, radiocarpal, mediocarpal and carpo-metacarpal joints can be well imaged and changes related to degenerative or erosive arthropathy detected. US can efficiently guide intraarticular injections (Lohman et al. 2007) under real time control. This helps in avoiding injury to adjacent structures such as nerves and vessels and in confirming the correct site of injection. US allows detection and assessment of several extrinsic articular ligaments as well as of the scapho-lunate ligament (Griffith et al. 2001; Jacobson et al. 2002; Finlay et al. 2004; Boutry et al. 2005; Taljanovic et al. 2008; Bihan et al. 2009; Renoux et al. 2009).

At the level of the dorsum of the hand and of the fingers, the ET can be followed till their distal insertion by US. The EPB is one of the thinnest tendons and inserts into the base of the proximal phalanx of the thumb. The two extensor carpi tendons (ECRB and ECRL) can be followed till their insertion into the base of the second and third metacarpals. The EPL

has a more complex course. At the distal radius, it reflects on the medial aspect of the Lister's tubercle, a bony ridge separating the third and the second compartment of the ET. Then, it points to the base of the thumb and overlies the ECRB and ECRL tendons. Finally, it joins the EPB at the level of the head of the first metacarpal to then insert into the base of the distal phalanx of the thumb. The EPL is then subject to local friction at two levels: at the Lister tubercle and when it crosses with the two extensor carpi tendons (De Maeseneer et al. 2005). The index has two extensor tendons, the communis and the indicis proprius, which runs medial to the communis. They have similar size and course. The EIP can be harvested and used as a tendon graft in several surgical procedures. The extensor digitorum communis tendons present a high variable organization at the dorsum of the hand related to presence of the so-called tendinous junctions. These are thin tendons directed obliquely and joining adjacent ET. The dorsal interossei muscles can be seen appreciated lying among the hyperechoic metatarsals.

At the level of the metacarpophalangeal joints, the ET are retained over the dorsal aspect of the joint by the sagittal bands, thin ligaments that prevent palmar displacement of the tendons during flexion of the fingers. These bands appear as thin hyperechoic laminae covering the tendons and inserting into the periphery of the capsule. At the level of the proximal phalanx, the ET of the 2–5 fingers split into a central band and two lateral bands. The central band inserts into the base of the middle phalanx while the lateral bands join into the midline to insert into the distal phalanx. The ET are well assessed by US at the level of the MCP joint. Their distal splitting is sometimes difficult to be appreciated at transverse images. Longitudinal images allow visualization of the insertion of the central band as well as of the distal insertion into the distal phalanx. Details of the insertion of the intrinsic muscles are not detected at US. The metacarpophalangeal and interphalangeal joints can be imaged in the sagittal and axial plane. US allows an accurate assessment of erosive articular changes (McNally 2008). The cartilage of the metacarpal and phalanx head can be judged by using a dorsal and palmar approach in the extended and flexed joint while the cartilage of the bases of the phalanges are not detectable at US. US examination performed during gentle stress of the fingers' joints can help in judging the capsuloligamentous complex. This is most

often performed at the level of the MCP of the thumb in the evaluation of tears of the ulnar collateral ligament.

4 Palmar Aspect

The palmar aspect of the wrist houses several tendons, nerves, and vessels (Figs. 9, 10, 11, 12, 13, 14, 15). Abbreviations for these structures are listed in Table 2. The most superficial and thinnest tendon is the PG that runs in the midline of the wrist within the subcutaneous tissue. The PG presents a high anatomic variability. It can be absent or be replaced by a muscle (palmaris inversus). In a deeper position, the flexor tendons of the fingers (FDS, FDP, FPL) run inside the carpal tunnel (CT), a fibrous tunnel made by the carpal bones (the floor) and a palmar thick ligament, the transverse carpal ligament (TCL) (the ceiling). Inside the CT, the tendons are surrounded by a common synovial sheath enveloping the FDS and FDP of the 2–5 fingers. This common sheath generally communicates with the digital sheath of the fifth finger. The 2–4 fingers have separate digital sheaths. The FPL has a separate long sheath extending from the CT till to the proximal phalanx of the thumb. The FCR, a strong tendon surrounded by its own synovial sheath, is also located inside the CT but runs in a separate lateral channel. In its distal portion, the FCR overlies the tubercle of the scaphoid and reflects over the palmar aspect of scapho-trapezio-trapezoid joint to deepen and reach its distal insertion into the base of the 2 and 3 metacarpals. The FCU is a straight tendon located at the medial aspect of the anterior face of the wrist that inserts into the proximal pole of the pisiform. Since it has a straight course this tendon is not surrounded by a synovial sheath but by its peritenon, a thin connective tissue lamina that facilitates its gliding. Besides several tendons, the CT houses also the MN, a flat nerve located just under the TCL at the radial aspect of the tunnel. The nerve has a close relation with the FDP and FDS of the index. It innervates the muscles of the thenar eminence as well as the 1st and 2nd lumbrical muscles. The MN is responsible for sensitivity of the first three fingers and radial aspect of the fourth finger. Details of its anatomy and anatomic variations will be discussed in more details in [Nerve Entrapment Syndromes](#). The Guyon's tunnel is a small fibroosseous tunnel located superficially and medially to the CT. It is delimited by the TCL and the lateral aspect of the pisiform (the roof) and the

Fig. 9 Palmar aspect. **a**, **c** Probe positioning for transverse examination. **b** Sonogram obtained as shown in **a**. *Sc* scaphoid, *P* pisiform, *FTs* flexor tendons, *white arrowhead* median nerve, *black arrowheads* transverse carpal ligament. **d** Sonogram obtained as shown in **c**. *Tr* trapezium, *H* hook of the hamate, *FTs* flexor tendons, *white arrowhead* median nerve, *black arrowheads* transverse carpal ligament

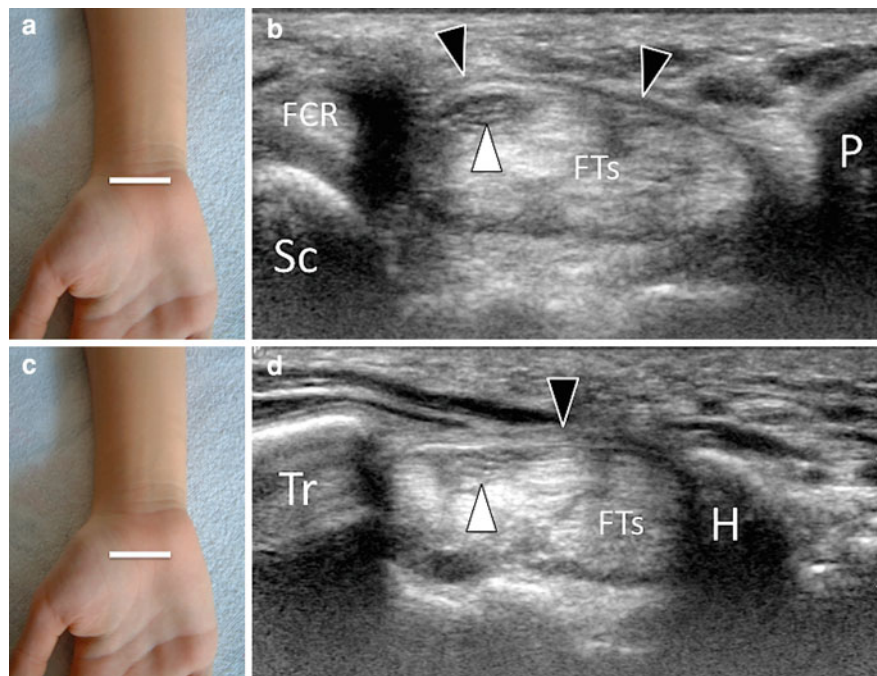


Fig. 10 Palmar aspect. **a**, **c** Probe positioning for transverse examination. **b** Sonogram obtained as shown in **a**. *FCUt* and *FCUm* tendon and muscle of the flexor carpi ulnaris, *white arrowhead* ulnar nerve, *black arrowhead* ulnar artery. **d** Sonogram obtained as shown in **c** (Guyon's tunnel). *Pis* pisiform, *CT* carpal tunnel, *white arrowhead* ulnar nerve, *black arrowhead* ulnar artery

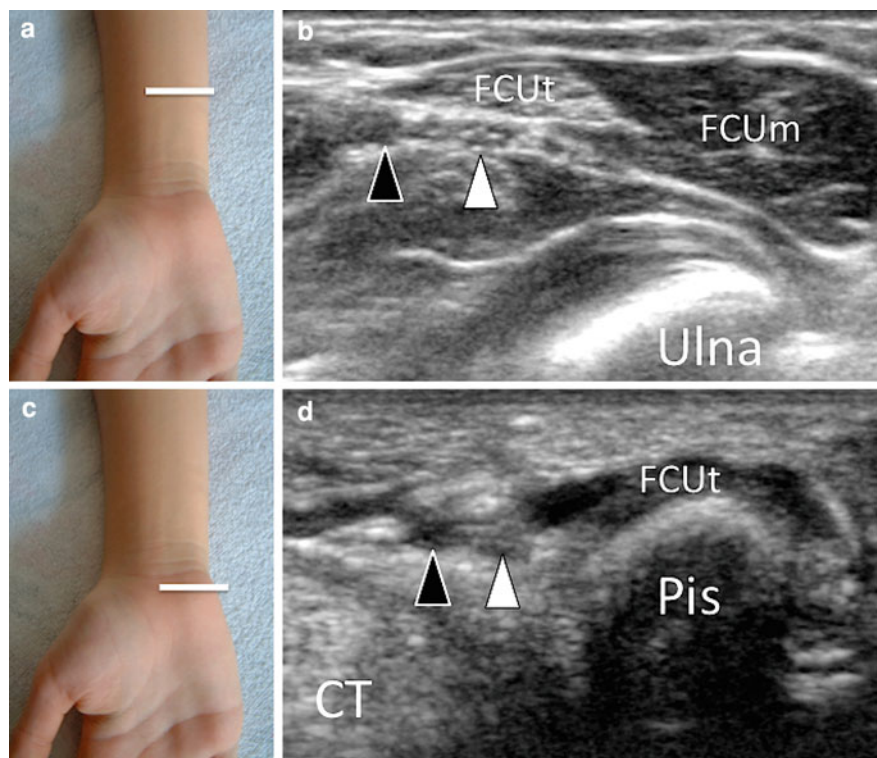
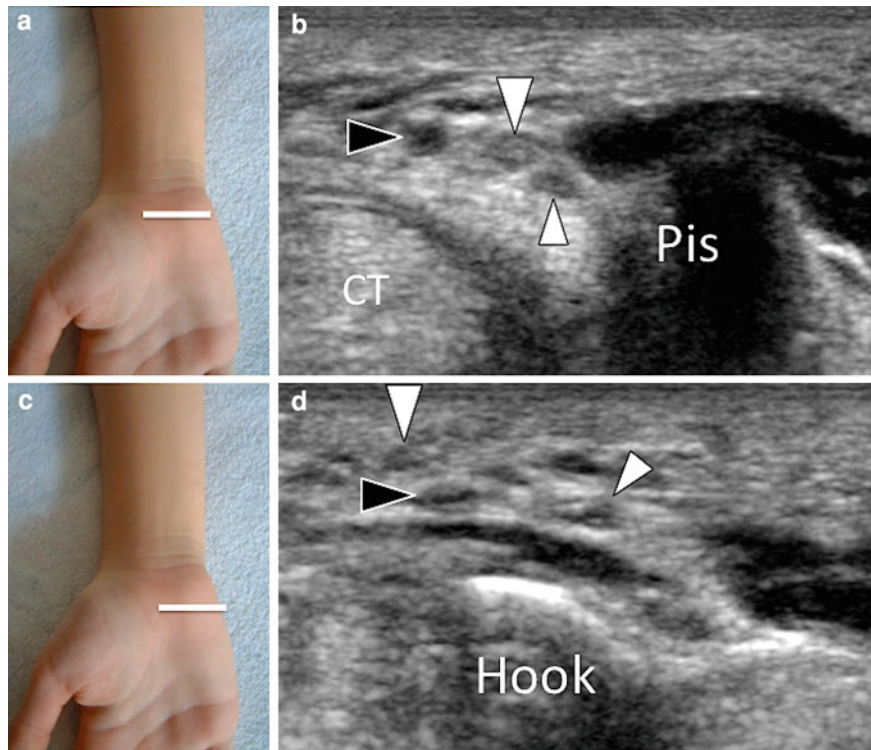


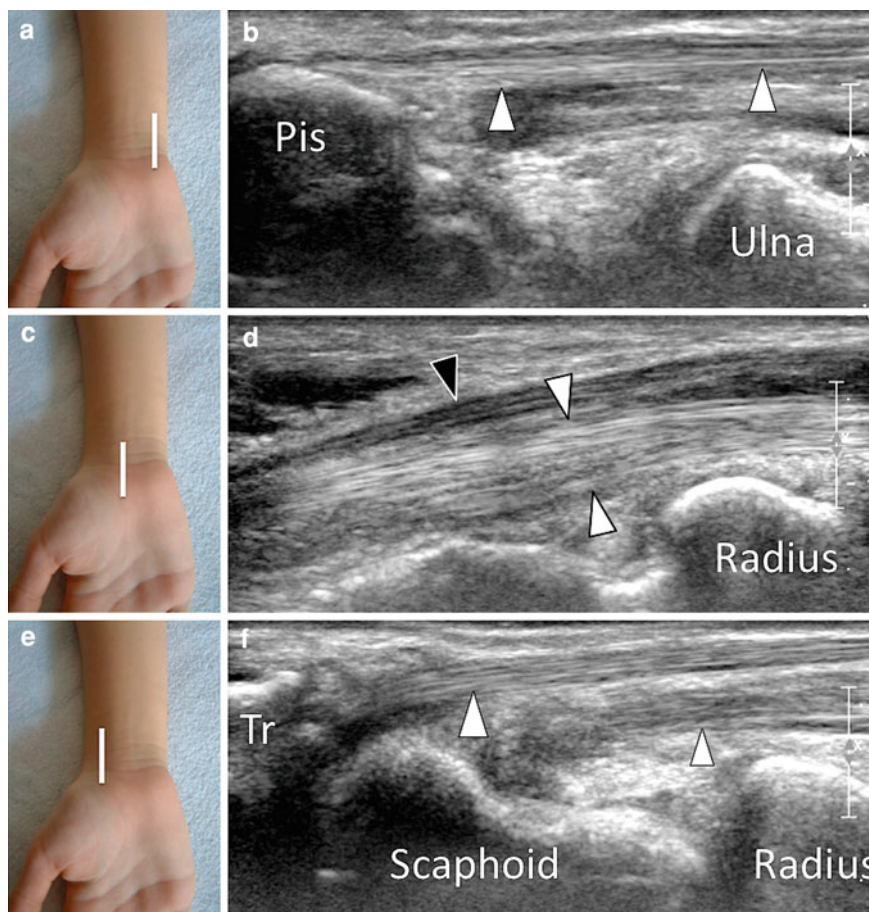
Fig. 11 Palmar aspect. **a, c** Probe positioning for transverse examination. **b** Sonogram obtained as shown in **a** (Guyon's tunnel). *Pis* pisiform, *CT* carpal tunnel, *large white arrowhead* superficial branch of the ulnar nerve, *small white arrowhead* deep branch of the ulnar nerve, *black arrowhead* ulnar artery. **d** Sonogram obtained as shown in **c** (Guyon's tunnel), *Hook* hook of the hamate bone, *large white arrowhead* superficial branch of the ulnar nerve, *small white arrowhead* deep branch of the ulnar nerve, *black arrowhead* ulnar artery



palmar carpal ligament (the ceiling). The tunnel houses, embedded by fat, the UN and the UAr surrounded by several UVE. The nerve is located between the artery and the pisiform. At variable level inside the tunnel or immediately distal to it, the UN splits in one motor branch and one or two sensitive branches. A more detailed description of the Guyon's anatomy will be presented in [Nerve Entrapment Syndromes](#). The UN is responsible for sensitivity of the fifth finger and medial aspect of the fourth finger. At the radial aspect of the wrist, the RAr is found running deep to the superficial fascia surrounded by satellite veins. The artery has close relation with the distal part of the sensitive branch of the RN. At the palm of the hand, the FDS and the FDP of the 2–5 fingers run together to join the base of the fingers. Their synovial sheaths are not detectable even when high-frequency transducers are used. The FDP, located just inferior to the FDS, give insertion to the lumbricals muscles. The vessels and the branches of the MN and UN run together located among the lumbricals muscles and the FDS surrounded by fat. More deeply are located the palmar interossei muscles. Utilization of high-frequency probes allows an optimal assessment of the anatomy of the flexor tendons at the

fingers. Transverse images show splitting of the FDS at the level of the proximal phalanx. The two tendinous laminae are located from proximal to distal: first superior, then lateral and medial and finally, inferior to the FDP tendon. They insert into the base of the middle phalanx. The FDP presents typically a triangular aspect with the base inferior in proximal scans and superior in more distal images. A frequent anatomic variation is bifidity of the FDP at the level of the distal part of the middle phalanx. This must not be interpreted as a posttraumatic longitudinal split. Longitudinal images are best suited to evaluate the tendons dynamically. When performed at the level of the MCP joint during flexion of the DIP joint, they show selective movements of the FDP tendon. Simultaneous flexion of the IPP joint allows concomitant movements of the FDS tendon. The insertion of the two FDS hemitendons can be imaged at the level of the intermediate phalanx by displacing the transducer medially and laterally. The insertion of the FDP into the base of the P3 is readily evident on sagittal images obtained over the distal phalanx. A variety of pulleys (annular and cruciform) retain the flexor tendons against the palmar aspect of the phalanges thus preventing palmar instability during

Fig. 12 Palmar aspect. **a, c, e** Probe positioning for longitudinal examination. **b, d, f** corresponding sonograms. **b** *Pis* pisiform, *white arrowheads* flexor carpi ulnaris tendon. **d** *Black arrowhead* median nerve, *white arrowheads* flexor digitorum tendons. **f** *Large white arrowhead* flexor carpi radialis tendon, *small white arrowhead* flexor pollicis longus tendon, *Tr* Trapezium



flexion (Bodner et al. 1999; Martinoli et al. 2000). Annular pulleys are quite rigid and are the main structures that prevent tendons bowstringing during flexion. They are numbered from 1 to 5 from proximal to, distal. The A2 and A4 pulleys located, respectively, at the base of P1 and P2 are functionally the most important. The annular pulleys are visualized as thin hyperechoic structures in longitudinal images. They show a normal thickening of their insertion in transverse images. The cruciform pulleys are more lax and located among the annular pulleys. They can be visualized at US only when a significant amount of fluid is present inside the tendon sheath.

The different joints of the fingers can be examined by sagittal and axial sonograms. The palmar plates are well depicted as hyperechoic structures, with homogeneous internal appearance, inserting into the base of the phalanges. Examination performed during gentle hyperextension of the examined joint can help in analysis of local tears or

avulsions. The palmar articular synovial recess is ready evident and must be analyzed for local effusion or synovial hypertrophy. Axial sonograms of the digital soft tissues allow assessment of the digital vessels and nerves till the level of the distal interphalangeal joint if high-frequency transducers are used.

5 Key Points

5.1 Advantages of Ultrasound in Wrist and Hand Assessment

- Ready available
- Non invasive
- Inexpensive
- Patient friendly
- Dynamic
- High resolution

Fig. 13 Palmar aspect. **a, c, e** Probe positioning. **b, d, f** Corresponding sonograms. **b** *1 Met* first metacarpal, *white arrowhead* flexor pollicis longus tendon. **d** *P1* proximal phalanx of the thumb, *S* sesamoid bone, *white arrowhead* flexor pollicis longus tendon. *F* *Fts* flexor tendons, *L* lumbrical muscle, *PIM* palmar interosseous muscles, *Met* metacarpal, *white arrowhead* common palmar digital artery, *black arrowhead* palmar digital nerve

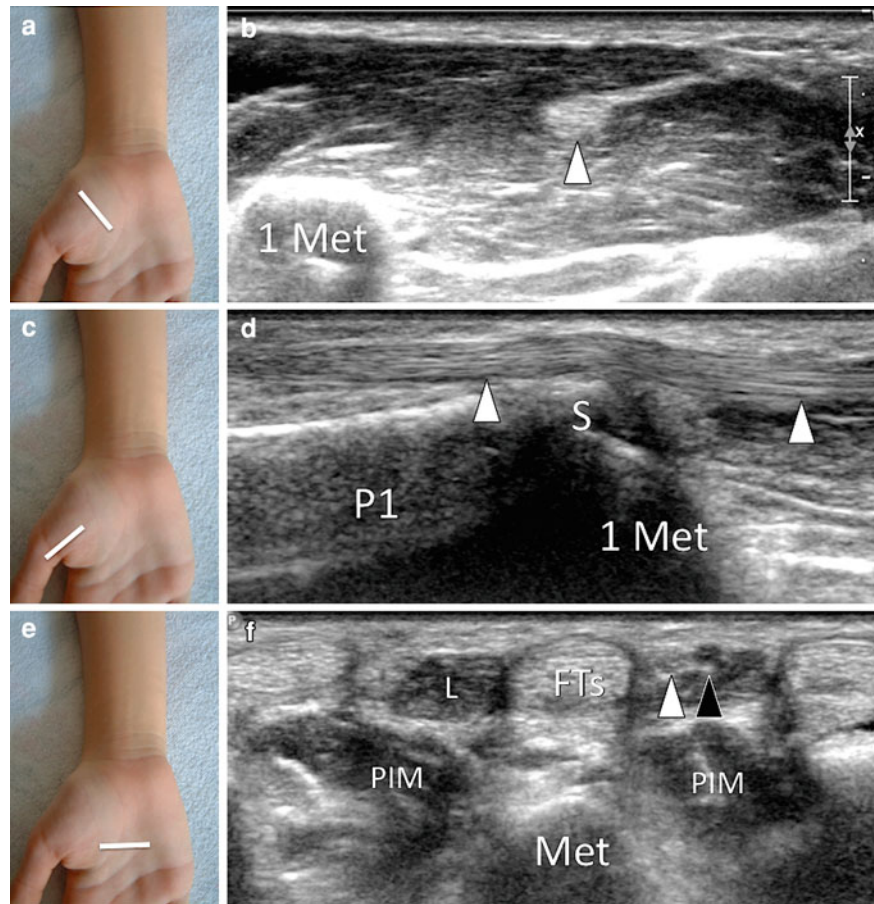
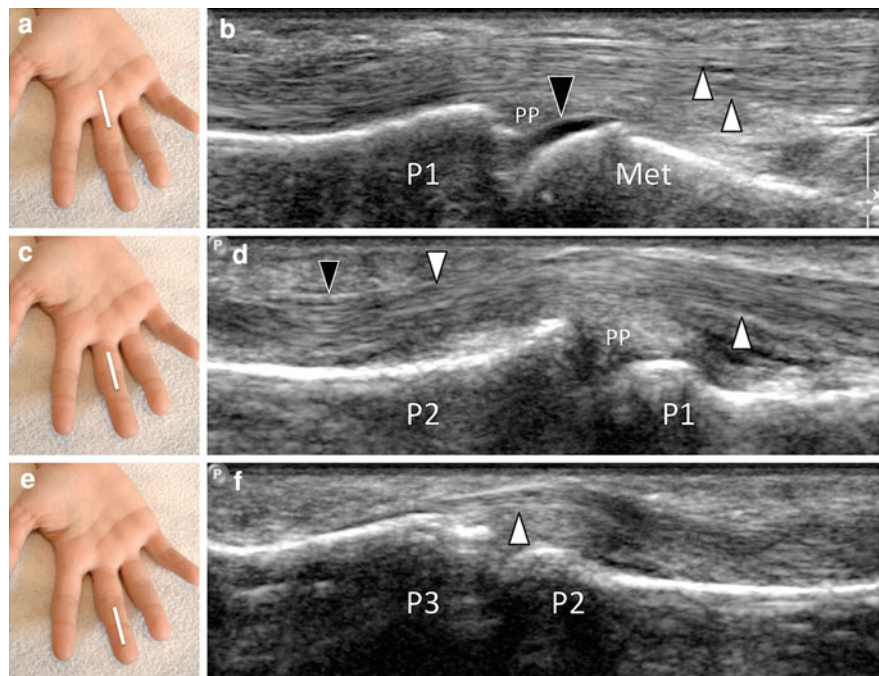


Fig. 14 Palmar aspect. **a, c, e** Probe positioning for longitudinal examination. **b, d, f** corresponding sonograms. **b** *Met* metacarpal, *P1* proximal phalanx, *PP* palmar plate, *white arrowheads* flexor digitorum superficialis and profundus tendons, *large black arrowhead* cartilage of the metacarpal head. **d** *P2* middle phalanx, *white arrowheads* flexor digitorum superficialis and profundus tendons, *small black arrowhead* A4 annular pulley. **f** *P3* distal phalanx, *white arrowhead* flexor digitorum profundus tendon



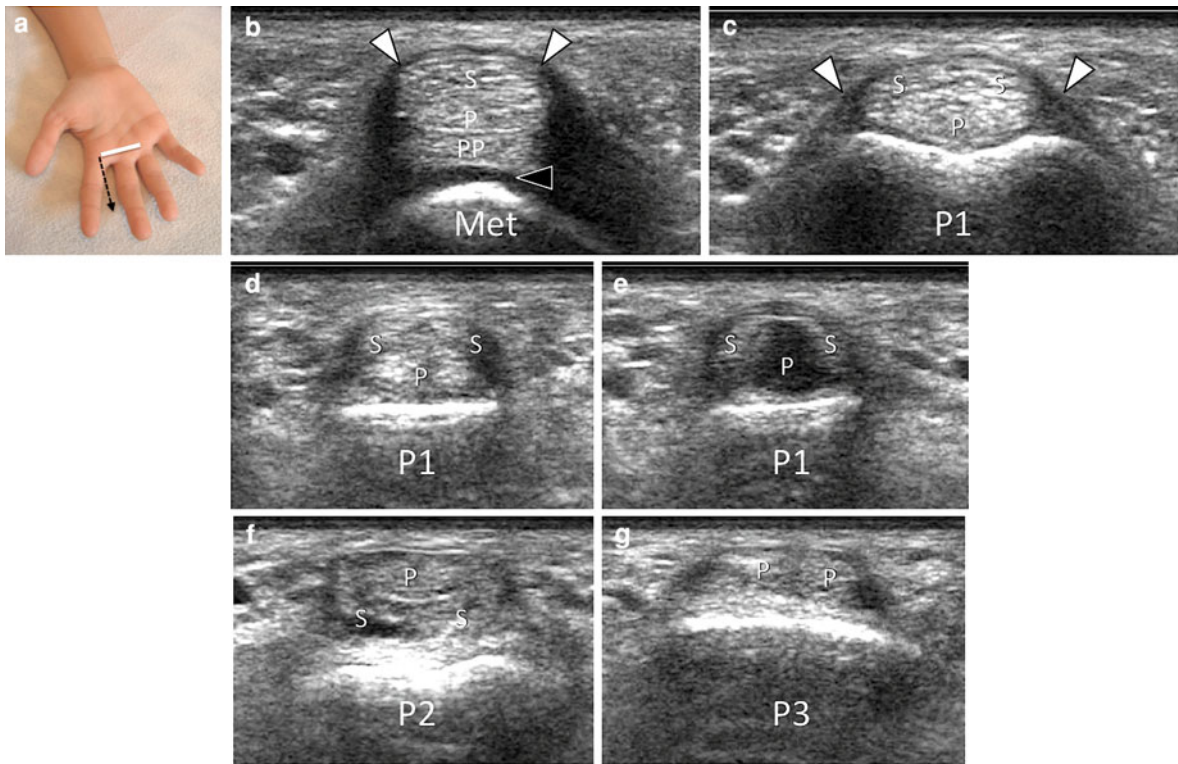


Fig. 15 Palmar aspect. **a** Probe positioning for transverse examination. **b-g** corresponding sonograms obtained from proximal to distal. **b-g** White arrowheads Annular pulleys, S flexor digitorum superficialis tendon, P flexor digitorum

profundus tendon, PP palmar plate of the metacarpophalangeal joint, black arrowhead cartilage of the metacarpal head, Met metacarpal, P1 proximal phalanx, P2 middle phalanx, P3 distal phalanx

Table 2 Anatomic structures of the palmar aspect of the wrist

<i>Flexor tendons</i>
PG = palmaris gracilis
FDS = flexor digitorum superficialis
FDP = flexor digitorum profundus
FPL = flexor pollicis longus
FCR = flexor carpi radialis
FCU = flexor carpi ulnaris
<i>Nerves</i>
MN = median nerve
UN = ulnar nerve
RN = radial nerve
<i>Vessels</i>
RAr = radial artery
RVe = radial veins
UAr = ulnar artery
UVe = ulnar veins

5.2 Disadvantages of Ultrasound in Wrist and Hand Assessment

- Long learning curve
- Operator dependent
- Partial assessment of cartilages, ligaments and bones

5.3 Operator Requisites for US Examination in Wrist and Hand Assessment

- Perfect knowledge of the normal anatomy and anatomic variants
- Clinical knowledge of the main disorders affecting the wrist and hand
- Use of accurate and standardized technique of examination

5.4 Basic Principles of US Technique of Examination in Wrist and Hand Assessment

- Perform a basic clinical examination of the affected area and review other imaging studies before starting the US examination
- Focus the examination on the basis of clinical findings
- Analyze the structures using multiple planes of scanning
- Perform dynamic examination and color Doppler examination
- Bilateral examination if required

References

- Backhaus M, Kamradt T, Sandrock D et al (1999) Arthritis of the finger joints: a comprehensive approach comparing conventional radiography, scintigraphy, ultrasound, and contrast-enhanced magnetic resonance imaging. *Arthritis Rheum* 42:1232–1245
- Backhaus M, Burmester G-R, Sandrock D et al (2002) Prospective two-year follow-up study comparing novel and conventional imaging procedures in patients with arthritic finger joints. *Ann Rheum Dis* 61:895–904
- Bianchi S, Martinoli C (2007) *Ultrasound of the musculoskeletal system*. Springer, Heidelberg
- Bianchi S, Martinoli C, Abdelwahab IF (1999) High-frequency ultrasound examination of the wrist and hand. *Skeletal Radiol* 28:121–129
- Bianchi S, Martinoli C, Sureda D et al (2001) Ultrasound of the hand. *Eur J Ultrasound* 14:29–34
- Bianchi S, Martinoli C, Montet X et al (2003) Wrist and hand ultrasound. *Radiologe* 43:831–840
- Bihan M, Pesquer L, Meyer P et al (2009) High resolution sonography of the dorsal radiocarpal and intercarpal ligaments: findings in healthy subjects with anatomic correlation to cadaveric wrists. *J Radiol* 90:813–817
- Blomley MJ, Cooke JC, Unger EC et al (2001) Microbubble contrast agents: a new era in ultrasound. *BMJ* 322:1222–1225
- Bodner G, Rudish A, Gabl M et al (1999) Diagnosis of digital flexor tendon annular pulley disruption: comparison of high frequency ultrasound and MRI. *Ultraschall Med* 20:131–136
- Boutry N, Lapegue F, Masi L et al (2005) Ultrasonographic evaluation of normal extrinsic and intrinsic carpal ligaments: preliminary experience. *Skeletal Radiol* 34:513–521
- Brasseur J-L, Tardieu M (2006) *Echographie de l'appareil locomoteur*. Masson, Paris
- Chiou HJ, Chou YH, Chang CY (2001) Ultrasonography of the wrist. *Can Assoc Radiol J* 5:302–311
- Creteur V, Peetrons P (2000) Ultrasonography of the wrist and the hand. *J Radiol* 81:346–352
- De Maeseneer M, Marcelis S, Osteaux M et al (2005) Sonography of a rupture of the tendon of the extensor pollicis longus muscle: initial clinical experience and correlation with findings at cadaveric dissection. *AJR Am J Roentgenol* 184:175–179
- De Maeseneer M, Marcelis S, Jager T et al (2009) Spectrum of normal and pathologic findings in the region of the first extensor compartment of the wrist: sonographic findings and correlations with dissections. *J Ultrasound Med* 28:779–786
- Ferrara MA, Marcelis S (1997) Ultrasound examination of the wrist. *J Belge Radiol* 80:78–80
- Finlay K, Lee R, Friedman L (2004) Ultrasound of intrinsic wrist ligament and triangular fibrocartilage injuries. *Skeletal Radiol* 33:85–90
- Goldberg BB, Liu JB, Forsberg F (1994) Ultrasound contrast agents: a review. *Ultrasound Med Biol* 20:319–333
- Grassi W, Tittarelli E, Pirani O et al (1993) Ultrasound examination of metacarpophalangeal joints in rheumatoid arthritis. *Scand J Rheumatol* 22:243–247
- Griffith JF, Chan DP, Ho PC et al (2001) Sonography of the normal scapholunate ligament and scapholunate joint space. *J Clin Ultrasound* 29:223–229
- Jacobson JA, Oh E, Propeck T et al (2002) Sonography of the scapholunate ligament in four cadaveric wrists: correlation with MR arthrography and anatomy. *AJR Am J Roentgenol* 179:523–527
- Karim Z, Wakefield RJ, Conaghan PG et al (2001) The impact of ultrasonography on diagnosis and management of patients with musculoskeletal conditions. *Arthritis Rheum* 44:2932–2933
- Koski JM (1992) Ultrasonography in the detection of effusion in the radiocarpal and midcarpal joints. *Scand J Rheumatol* 21:79–81
- Lee JC, Healy JC (2005) Normal sonographic anatomy of the wrist and hand. *Radiographics* 25:1577–1590
- Lohman M, Vasenius J, Nieminen O (2007) Ultrasound guidance for puncture and injection in the radiocarpal joint. *Acta Radiol* 48:744–747
- Martinoli C, Bianchi S, Derchi L et al (2000) Sonographic evaluation of digital annular pulleys tears. *Skeletal Radiol* 29:387–391
- McNally E (2004) *Practical musculoskeletal ultrasound*. Elsevier, Amsterdam
- McNally EG (2008) Ultrasound of the small joints of the hands and feet: current status. *Skeletal Radiol* 37:99–113
- Middleton WD, Teefey SA, Boyer MI (2001) Hand and wrist sonography. *Ultrasound Q* 17:21–36
- Milbradt H, Calleja Cancho E, Qaiyumi SA et al (1990) Sonography of the wrist and the hand. *Radiologe* 30:360–365
- Moschilla G, Bredahl W (2002) Sonography of the finger. *AJR* 178:1451–1457
- Muncibi F, Carulli C, Paez DC et al (2008) A case of bilateral extensor digitorum brevis manus. *Chir Organi Mov* 92:133–135
- Read JW, Conolly WB, Lanzetta M et al (1996) Diagnostic ultrasound of the hand and wrist. *J Hand Surg* 21:1004–1010
- Renoux J, Zeitoun-Eiss D, Brasseur JL (2009) Ultrasonographic study of wrist ligaments: review and new perspectives. *Semin Musculoskelet Radiol* 13:55–65
- Robertson BL, Jamadar DA, Jacobson JA et al (2007) Extensor retinaculum of the wrist: sonographic characterization and

- pseudotenosynovitis appearance. *AJR Am J Roentgenol* 188:198–202
- Scheel AK, Hermann KG, Ohrndorf S et al (2006) Prospective long term follow-up imaging study comparing radiography, ultrasonography and magnetic resonance imaging in rheumatoid arthritis finger joints. *Ann Rheum Dis* 65:595–600
- Szkudlarek M, Narvestad E, Klarlund M et al (2004a) Ultrasonography of the metatarsophalangeal joints in rheumatoid arthritis: comparison with magnetic resonance imaging, conventional radiography, and clinical examination. *Arthritis Rheum* 50:2103–2112
- Szkudlarek M, Narvestad E, Court-Payen M et al (2004b) Ultrasonography of the RA finger joints is more sensitive than conventional radiography for detection of erosions without loss of specificity, with MRI as a reference method. *Ann Rheum Dis* 63:82–83
- Tagliafico A, Rubino M, Autuori A et al (2007) Wrist and hand ultrasound. *Semin Musculoskelet Radiol* 11:95–104
- Taljanovic MS, Sheppard JE, Jones MD et al (2008) Sonography and sonoarthrography of the scapholunate and lunotriquetral ligaments and triangular fibrocartilage disk: initial experience and correlation with arthrography and magnetic resonance arthrography. *J Ultrasound Med* 27:179–191
- Teefey SA, Middleton WD, Boyer MI (2000) Sonography of the hand and wrist. *Semin Ultrasound CT MR* 21:192–204
- Terslev L, Torp-Pedersen S, Sarnik A et al (2003) Doppler ultrasound and magnetic resonance imaging of synovial inflammation of the hand in rheumatoid arthritis: a comparative study. *Arthritis Rheum* 48:2434–2441
- Tubbs RS, Stetler W, Kelly DR et al (2007) Acrel's ganglion. *Surg Radiol Anat* 29:379–381
- Van Holsbeeck M, Introcaso JH (2001) *Musculoskeletal ultrasound*, 2nd edn. Mosby Co, St Louis
- Wakefield RJ, Gibbon WW, Conaghan PG et al (2000) The value of sonography in the detection of bone erosions in patients with rheumatoid arthritis. *Arthritis Rheum* 43:2762–2770
- Walther M, Harms H, Krenn V et al (2001) Correlation of power Doppler sonography with vascularity of the synovial tissue of the knee joint in patients with osteoarthritis and rheumatoid arthritis. *Arthritis Rheum* 44:331–829